

Genetic Engineering of Hematopoiesis for Targeted IFN- α Delivery Inhibits Breast Cancer Progression

Giulia Escobar,^{1,2} Davide Moi,^{2*} Anna Ranghetti,² Pinar Ozkal-Baydin,² Mario Leonardo Squadrito,^{1,2†} Anna Kajaste-Rudnitski,² Attilio Bondanza,^{1,3} Bernhard Gentner,^{1,2} Michele De Palma,^{2†} Roberta Mazzeri,^{2*‡} Luigi Naldini^{1,2‡§}

The immunosuppressive tumor microenvironment represents a major hurdle to cancer therapy. We developed a gene transfer strategy into hematopoietic stem cells (HSCs) to target transgene expression to tumor-infiltrating monocytes/macrophages. Using a combination of transcriptional and microRNA-mediated control, we achieved selective expression of an interferon- α (IFN- α) transgene in differentiated monocytes of human hematohimeric mice. We show that IFN- α transgene expression does not impair engraftment and long-term multilineage repopulation of NSG (NOD/LtSz-scidIL2R γ^{null}) mice by transplanted human HSCs. By providing a source of human cytokines in the mice, we improved the functional reconstitution of human myeloid, natural killer, and T cell lineages, and achieved enhanced immune-mediated clearance of transplanted human breast tumors when hematopoiesis was engineered for tumor-targeted IFN- α expression. By applying our strategy to mouse breast cancer models, we achieved inhibition of tumor progression and experimental metastases in an autologous setting, likely through enhanced generation of effector T cells and their recruitment to the neoplastic tissues. By forcing IFN- α expression in tumor-infiltrating macrophages, we blunted their innate protumoral activity and reprogrammed the tumor microenvironment toward more effective dendritic cell activation and immune effector cell cytotoxicity. Overall, our studies validate the feasibility, safety, and therapeutic potential of a new cancer gene therapy strategy, and open the way to test this approach as adjuvant therapy in advanced breast cancer patients.

INTRODUCTION

Increasing evidence shows that the immune system has the potential to contribute to cancer eradication (1). The graft-versus-tumor activity of donor T cells is exploited in allogeneic hematopoietic stem cell (HSC) transplantation to treat refractory hematological malignancies (2). More recently, several immunotherapeutic approaches aimed at promoting antitumor immunity have shown promising results in the treatment of advanced solid tumors (3). However, a major hurdle to the efficacy of cancer immunotherapy is the immunosuppressive tumor microenvironment, which counteracts effective and long-lasting antitumor responses through the release of inhibitory factors for innate and adaptive immune cells and the recruitment of immunosuppressive leukocytes (4). Thus, approaches aiming at reprogramming the tumor microenvironment toward a more permissive state for the generation and deployment of immune effector responses are crucial to improve the success of current immunotherapy strategies for cancer.

Type I interferons (IFNs) are pleiotropic cytokines involved in innate and adaptive immunity that have been shown to promote antitumor immune responses (5). IFNs promote the survival, proliferation,

and cytotoxicity of CD8⁺ T cells, the immunoglobulin class switching of B cells, and the activation of dendritic cells (DCs), which have a crucial role in the initiation of adaptive immune responses (6, 7). Moreover, IFNs increase natural killer (NK) cell cytotoxicity by modulating the surface expression of activating and inhibitory receptors and enhance NK cell survival and expansion by inducing the production of interleukin-15 (IL-15), a cytokine also important to maintain CD8⁺ memory T cells. Type I IFNs also increase the expression of tumor antigens on neoplastic cells, making them more immunogenic (8). The broad biological activities of IFNs provided the rationale for testing administration of exogenous IFN- α as an anticancer treatment, which proved effective against several solid and hematological malignancies (9). However, clinical use of IFN- α has since declined because of the substantial toxicity associated with systemic administration and the limited efficacy at the maximal tolerated doses, thus calling for safer and more effective delivery strategies (10).

Our group has described a population of monocytes, TIE2-expressing monocytes (TEMs), which have proangiogenic activity and are preferentially recruited to tumors in mice and humans (11, 12). We exploited the tumor-homing ability of TEMs to target IFN- α to mouse tumors by transplanting hematopoietic stem/progenitor cells (HS/PCs), which were genetically modified with a transcriptionally targeted IFN- α transgene using enhancer/promoter sequences from the mouse *Tie2/Tek* gene (13). Whereas this study provided proof of principle of a potential new therapeutic strategy, its translation to the clinical setting has remained challenging because of concerns on the feasibility and safety of gene transfer into human HSCs.

Recently, we and others have provided evidence for safe and effective HSC gene transfer by lentiviral vectors (LVs) in clinical trials of gene therapy for inherited monogenic diseases (14–17), thus opening

¹Vita-Salute San Raffaele University, 20132 Milan, Italy. ²Angiogenesis and Tumor Targeting Research Unit and San Raffaele Telethon Institute for Gene Therapy, San Raffaele Scientific Institute, 20132 Milan, Italy. ³Leukemia Immunotherapy Unit, San Raffaele Scientific Institute, 20132 Milan, Italy.

*Present address: The University of Queensland Diamantina Institute, Translational Research Institute, Brisbane, Queensland 4102, Australia.

†Present address: The Swiss Institute for Experimental Cancer Research (ISREC), School of Life Sciences, Swiss Federal Institute of Technology Lausanne (EPFL), Lausanne 1015-CH, Switzerland.

‡These authors share senior authorship.

§Corresponding author. E-mail: naldini.luigi@hsr.it

the way to clinical development of our anticancer strategy. However, transfer of an IFN- α transgene into HS/PCs raises further concerns, given the well-known detrimental effects of high-dose IFN- α on myelothrombopoiesis (18) and the reported activation of dormant HSCs in IFN- α -treated mice, ultimately leading to exhaustion of the HSC pool (19). Thus, we sought to implement a stringent control of transgene expression during posttransplant hematopoiesis to limit HSC exposure to transgenic IFN- α expression, and performed comprehensive preclinical studies to establish the safety and potential efficacy of the strategy.

RESULTS

Genetic engineering of HSCs for targeted transgene expression in myelo-monocytic progeny

To express the human IFN- α specifically in human TEMs (12), we cloned enhancer/promoter sequences from the human *TIE2/TEK* locus with homology to the sequences previously described from the mouse genome (20) into a third-generation, green fluorescent protein (GFP)-expressing lentiviral reporter vector (Fig. 1A) and confirmed the selective activity of this promoter in endothelial cells (fig. S1, A

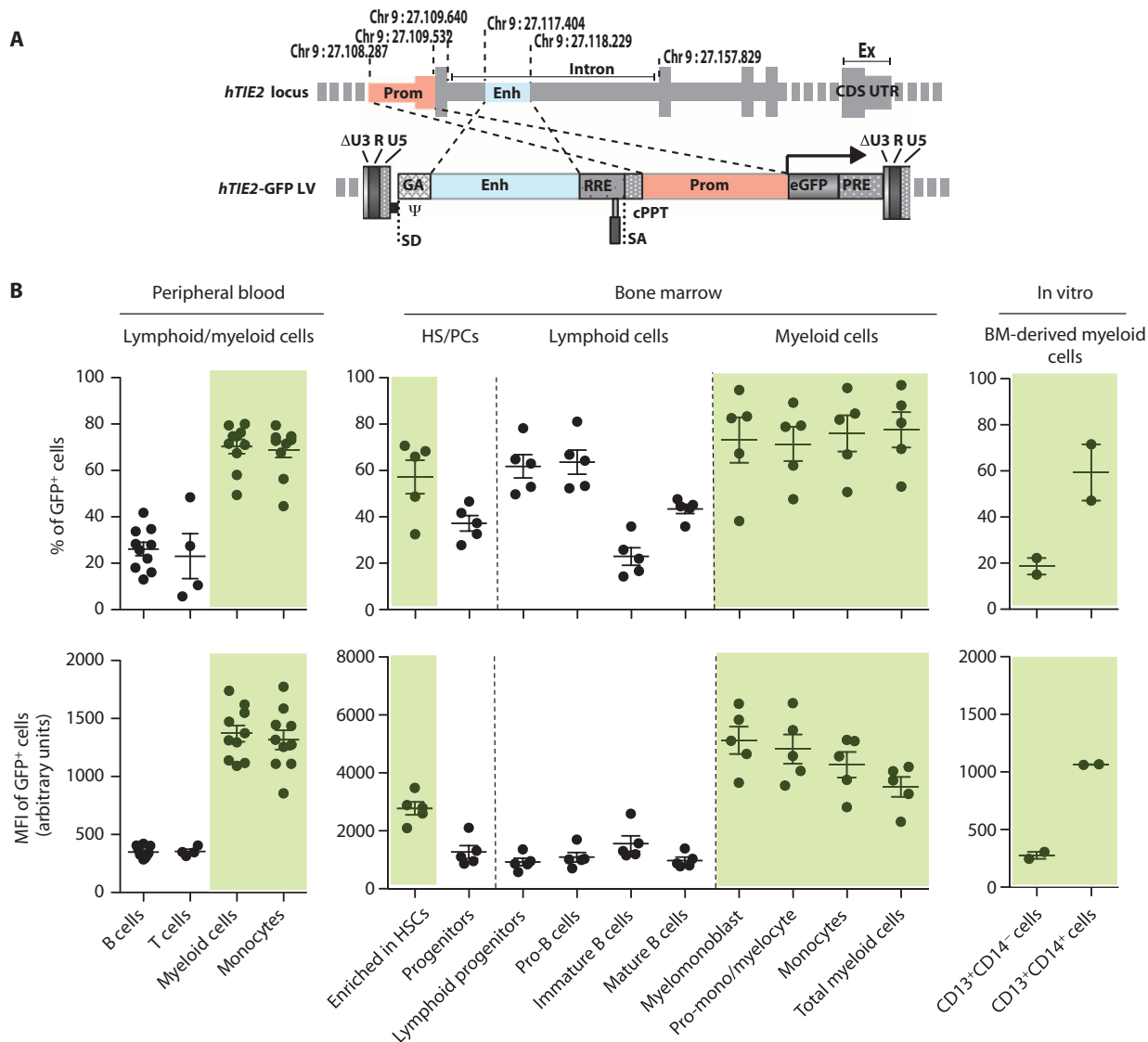
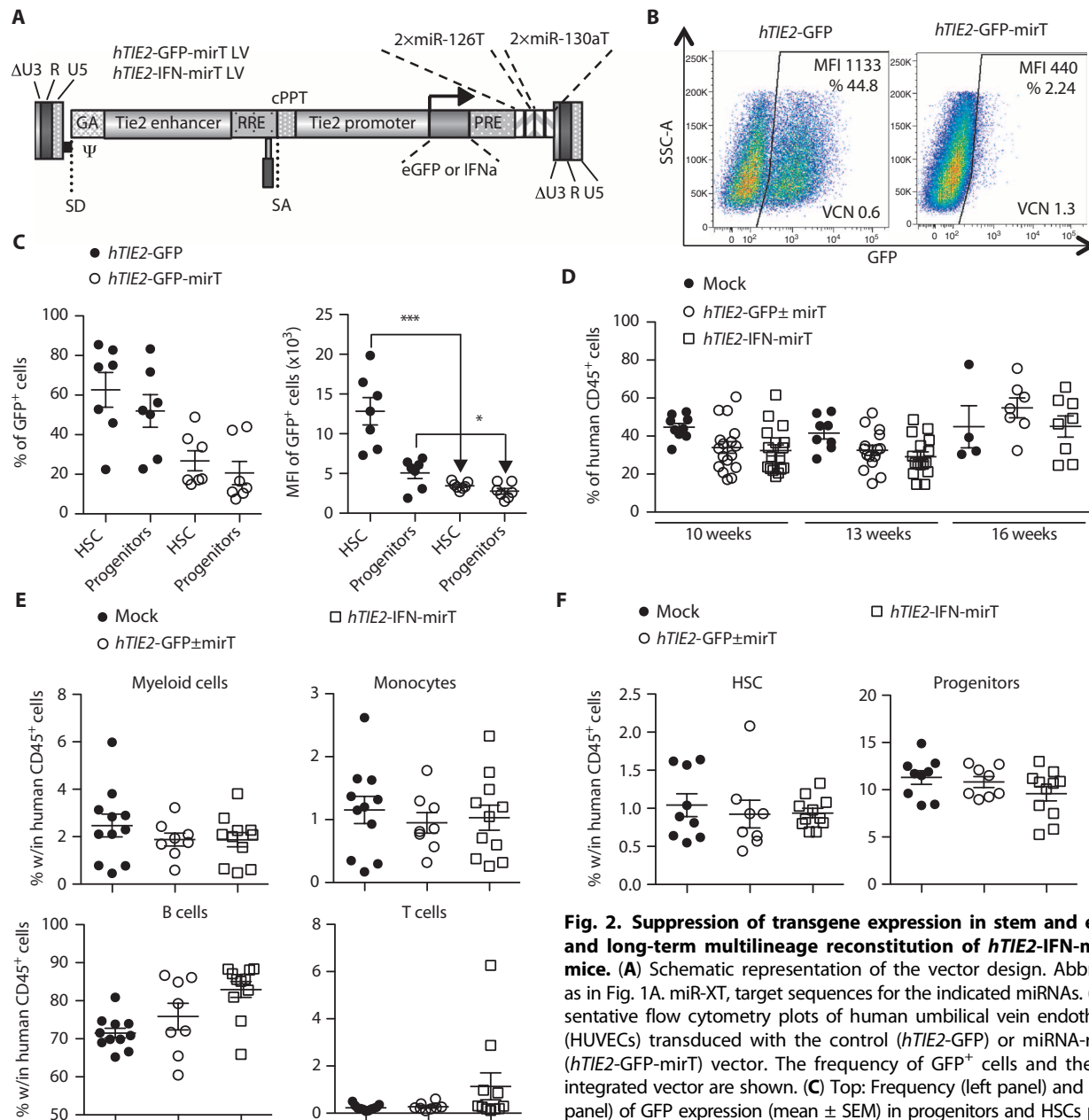


Fig. 1. Targeted transgene expression in the myelo-monocytic progeny of HS/PCs by an LV exploiting the human *TIE2* gene regulatory sequences. (A) Schematic representation of the vector design and of the human *TIE2* locus. The genomic coordinates of the human *TIE2* promoter and enhancer are indicated. Prom, promoter; Enh, enhancer; Ex, exon; CDS, coding sequence; UTR, untranslated region. Δ U3 R U5, long terminal repeat regions with self-inactivating deletion in U3; ψ , packaging signal; eGFP, enhanced green fluorescent protein; SD and SA, splicing donor and acceptor sites; RRE, Rev-

responsive element; cPPT, central polypurine tract; PRE, posttranscriptional regulatory element of woodchuck hepatitis virus. (B) Frequency (top panel) and level (MFI; bottom panel) of GFP expression (mean \pm SEM) in the indicated hematopoietic populations of *hTIE2-GFP* NSG mice ($n = 4$ to 10) or after in vitro differentiation of human CD34⁺ cells derived from the BM of *hTIE2-GFP* NSG mice. The populations in which the *TIE2* promoter is expected to be active are highlighted in green. Note that GFP MFI cannot be directly compared among the three plots, as they represent distinct experimental acquisitions.



0.0134, *** $P = 0.0002$, Student's t test. (D) Percentages of human CD45⁺ cells (mean \pm SEM) present in the peripheral blood (PB) of mock ($n = 4$ to 9), *hTIE2-GFP-miRt* ($n = 7$ to 17), and *hTIE2-IFN-miRt* ($n = 8$ to 17) NSG mice at the indicated time points after transplant. (E) Percentages within human CD45⁺ cells (mean \pm SEM) of the indicated lineages present in the PB of mock ($n = 11$), *hTIE2-GFP-miRt* ($n = 8$), and *hTIE2-IFN-miRt* ($n = 11$) NSG mice at 12 weeks after transplant. (F) Percentages within human CD45⁺ cells (mean \pm SEM) of HSCs and progenitors present in the BM of mock ($n = 9$), *hTIE2-GFP-miRt* ($n = 8$), and *hTIE2-IFN-miRt* ($n = 11$) NSG mice at 19.5 weeks after transplant.

to C). We then transduced CD34⁺ HS/PCs from human cord blood and grew them in clonogenic assays. Myeloid (CD33⁺), but not erythroid (CD235a⁺), cells expressed the GFP protein (fig. S1D). To investigate the specificity of expression of the *hTIE2-GFP* LV throughout hematopoiesis, we used a human hematochimeric xenotransplantation model. We transduced human CD34⁺ HS/PCs with the *hTIE2-GFP* LV, transplanted them in NOD/LtSz-scidIL2Rγ^{null} (NSG) mice (21, 22), and analyzed hematopoietic subpopulations derived from the reconstituted

human hematopoiesis (figs. S2 and S3). We found a strong preferential expression of the *hTIE2-GFP* LV in circulating myeloid versus lymphoid cells, as shown by the frequency and mean fluorescence intensity (MFI) of GFP⁺ cells (Fig. 1B; overall MFI fold difference \pm SEM, 10 ± 1.4 ; see Supplementary Materials and Methods for calculation). Correspondingly, in the bone marrow (BM), GFP expression was well detectable in differentiating myeloid cells, but not in lymphoid cells or in CD34⁺CD38⁺ progenitors. GFP expression was also detectable in the

early progenitor subset enriched for HSCs (CD34⁺CD38⁻), which express the TIE2 receptor (23).

Because circulating myeloid cells may not reach full maturation in NSG mice, we investigated if the expression of our LV was enhanced upon terminal monocyte/macrophage differentiation. We cultured *in vitro* human CD34⁺ cells isolated from the BM of transplanted NSG mice in the presence of macrophage colony-stimulating factor (M-CSF) and granulocyte colony-stimulating factor (G-CSF), and found strong GFP up-regulation in the differentiated CD14⁺ macrophages with respect to CD13⁺CD14⁻ granulocytic cells (Fig. 1B). Together, these results indicate that the reconstituted human *TIE2* regulatory elements are preferentially activated during myeloid differentiation and reach high activity in mature monocytes/macrophages. The expression cassette, however, is also active in HSC.

Detargeting transgene expression from HS/PCs

Because chronic activation of the type I IFN pathway in HSCs might impair their function (19, 24), we refined our strategy by incorporating target sequences for miR-126 and miR-130a (mirT) into the LV (Fig. 2A). This modification makes the LV susceptible to negative regulation (repression) by the endogenous microRNAs (miRNAs). We previously showed that both miR-126 and miR-130a are expressed in the HS/PC compartment but not in mature blood cells (25, 26). Because we inserted multiple copies of perfectly complementary miRNA target sequences in the vector, the miRNAs act as small interfering RNAs against the transcript and effectively suppress its translation. Thus, our miRNA-based off-switch design should detarget LV expression from HS/PCs, limiting potential transgene toxicity while enabling expression in their differentiated myelo-monocytic progeny.

To verify transgene detargeting in miR-126-expressing cells, we first transduced human umbilical vein endothelial cells (HUVECs), which express high levels of miR-126 (27), with both control (*hTIE2*-GFP) and miRNA-regulated (*hTIE2*-GFP-mirT) LVs. GFP was not expressed in cells transduced with the mirT vector (Fig. 2B), indicating full suppression of the *hTIE2*-mirT construct in endothelial cells. We then investigated posttranscriptional regulation of this construct in human HS/PC subpopulations in the BM of reconstituted NSG mice carrying matched amounts of *hTIE2*-GFP or *hTIE2*-GFP-mirT LV [vector copy number (VCN) = 2 to 5]. We found effective transgene detargeting from HSCs by the mirT LV [6.6 ± 1 (fold repression ± SEM); *P* = 0.0002, Student's *t* test; see Supplementary Materials and Methods for calculation] (Fig. 2C). The residual GFP expression observed in progenitors was also reduced by the mirT LV (4.1 ± 0.7, *P* = 0.0134), albeit to a lower extent than in HSCs, in agreement with the expression patterns of miR-126 and miR-130a, which peak in HSCs and decrease in progenitors (25, 26). These results indicate effective miRNA-mediated detargeting of transgene expression from the HS/PC compartment.

We then cloned the human *IFNA2B* complementary DNA (cDNA) in the *hTIE2*-GFP-mirT (*hTIE2*-IFN-mirT) and *hTIE2*-GFP (*hTIE2*-IFN) LVs (see Fig. 2A) and confirmed suppression of IFN- α expression in HUVECs transduced with the mirT-regulated vector by enzyme-linked immunosorbent assay (ELISA) (fig. S4A). We then tested whether transduction with the *hTIE2*-IFN-mirT LV would affect HS/PC properties. Clonogenic assays did not reveal IFN- α toxicity on committed progenitors (fig. S4B). Mice transplanted with *hTIE2*-IFN-mirT-transduced HS/PCs (*hTIE2*-IFN-mirT mice) showed similar engraftment levels and kinetics as compared to *hTIE2*-GFP-mirT and *hTIE2*-GFP (*hTIE2*-GFP±mirT) mice or mice transplanted with

mock-transduced HS/PCs (mock mice) (Fig. 2D). Furthermore, they showed similar proportions of human B, T, and myeloid cells in the blood and HS/PCs in the BM long-term posttransplant (Fig. 2, E and F) with no evidence of *in vivo* counterselection of *hTIE2*-IFN-mirT-transduced cells (fig. S4C). Together, these results indicate that transduction with the *hTIE2*-IFN-mirT LV did not interfere with the ability of human CD34⁺ cells to reconstitute a sustained multilineage hematopoietic system in NSG mice.

Activation of a type I IFN response in tumors of human hematochimeric mice

Having provided evidence of the feasibility of engineering human hematopoiesis with the new IFN- α LV, we sought to determine whether it could enable delivery of bioactive IFN- α to the tumor site and hence inhibit its growth. Thirteen weeks after the transplant of gene-modified human CD34⁺ cells, we orthotopically injected the MDA-MB 231 (MDA) breast cancer cell line in *hTIE2*-IFN-mirT (*n* = 10) and, as controls, *hTIE2*-GFP or *hTIE2*-GFP-mirT (*hTIE2*-GFP±mirT) (*n* = 13) or mock (*n* = 7) NSG mice (Fig. 3A). We noted an increase in the number of circulating human myeloid cells 3.5 weeks after tumor injection [4.7 ± 0.7 (fold change ± SEM) compared to tumor-free NSG mice], with the greatest expansion found in monocytes (7.6 ± 1.5) and no expansion seen in B cells (Fig. 3B). Mechanistically, such myeloid cell expansion may be induced by human G-CSF, a cytokine that promotes the proliferation and differentiation of myeloid progenitors (28) and that is produced by MDA cells (29). Indeed, flow cytometric analysis of tumor biopsies obtained 4.5 weeks after tumor injection showed that human hematopoietic cells were recruited into the tumors, and most of them were myeloid, with no differences between the treatment groups (Fig. 3C and fig. S5A). T cells were very few in the tumor as in the blood.

We then assessed whether the recruited myeloid cells could deliver IFN- α to the tumors and hence induce activation of a type I IFN response. We measured the expression of two IFN-inducible genes, *IRF7* and *OAS1A*, by quantitative polymerase chain reaction (qPCR) in the tumors, BM, and liver of *hTIE2*-IFN-mirT and control mice at 4.5 weeks after tumor injection. We found both genes to be significantly up-regulated in tumors of *hTIE2*-IFN-mirT mice compared to mock controls (Fig. 3D). These results indicate that the progeny of transduced and transplanted human HS/PCs infiltrated the tumor and induced an IFN- α response preferentially at the tumor site. Despite the observed activation of IFN- α signaling in the tumors, we found no difference in the growth of orthotopically injected tumors between *hTIE2*-IFN-mirT mice and controls (Fig. 3E). The lack of antitumor efficacy was, however, not unexpected; indeed, the antitumor activity of IFN- α is mainly mediated through its modulatory activities on immune cells, which are impaired in NSG mice (30).

Generation of a human tumor model to study immune responses in human hematochimeric mice

To overcome the absence of human cytokines supporting full development and function of T, NK, and myeloid cells in NSG mice, we engineered MDA cells for expression of human granulocyte-macrophage colony-stimulating factor (GM-CSF), IL-7, or IL-15 (MDA3; fig. S6, A and B). When human NSG mice previously reconstituted with human hematopoietic cells were challenged with MDA3 cells, we observed a marked expansion of T and NK cells (fig. S7, A and B). Monocytes, which largely accounted for the myeloid cell expansion in MDA-injected mice, were not expanded. Conversely, in MDA3-injected mice, another

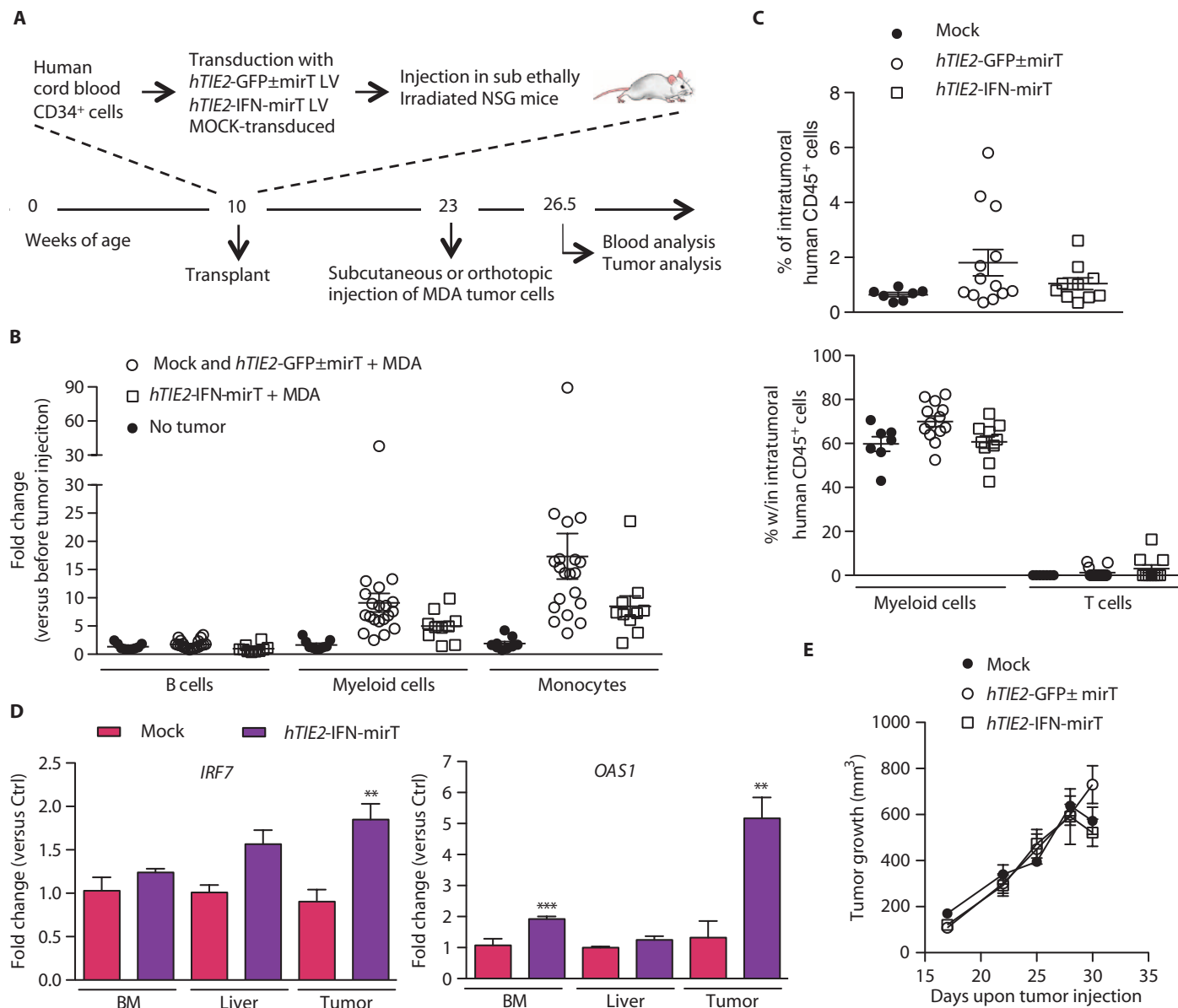


Fig. 3. Injection of MDA-MB 231 breast cancer cells into human hematochimeric NSG mice. (A) Schematic representation of the experimental design. (B) Fold change (mean ± SEM) of the absolute numbers of the indicated human cells at 3.5 weeks upon tumor injection with respect to T₀ (before tumor injection) in the PB of tumor-bearing (mock/*hTIE2*-GFP/*TIE2*-GFP-mirT, *n* = 20; *hTIE2*-IFN-mirT, *n* = 10) and tumor-free (no tumor, *n* = 9) human hematochimeric NSG mice. (C) Percentages (mean ± SEM) of total intratumoral human CD45⁺ cells (top panel) and of myeloid and T cells within intratumoral human CD45⁺ cells (bottom panel) in mock (*n* = 7),

hTIE2-GFP and *hTIE2*-GFP-mirT (*n* = 13), and *hTIE2*-IFN-mirT (*n* = 10) NSG mice at 4.5 weeks upon tumor injection. (D) *IRF7* (left) and *OAS1* (right) expression (mean fold change over Ctrl organs ± SEM) in tumors and organs of control (mock, *n* = 4) and IFN-treated (*hTIE2*-IFN-mirT, *n* = 10) human hematochimeric NSG mice, as measured by reverse transcription (RT)-qPCR. ***P* = 0.0045 (*IRF7*), ****P* = 0.0057 (*OAS1*), ****P* = 0.0007, Student's *t* test. (E) Tumor kinetic growth over time of orthotopically injected MDA-MB 231 cells (mean tumor measurement ± SEM) in *hTIE2*-GFP and *hTIE2*-GFP-mirT (*n* = 4), *hTIE2*-IFN-mirT (*n* = 3), and mock (*n* = 3) NSG mice.

myeloid cell population, characterized by high granularity (SSC^{high}) and lack of the monocyte marker CD14, primarily accounted for the expansion of the myeloid compartment (fig. S7C).

By monitoring tumor growth over time, we observed tumor regression in MDA3-injected as compared to MDA-injected mice (*P* = 0.0138, day 21, Student's *t* test; Fig. 4A). Notably, we found no significant difference in the growth of the two tumor cell lines orthotopically injected in untrans-

planted NSG mice, indicating that the transduced cytokines did not confer growth advantage or disadvantage on the MDA tumor cell line per se. Rather, this finding suggested that cytokine-primed human hematopoietic cells promoted tumor rejection. We then purified T cells from the mouse spleen and stimulated them in vitro. Whereas T cells from MDA-injected mice did not survive in culture, the T cells from MDA3-injected mice expanded and responded to restimulation with phytohemagglutinin (PHA)

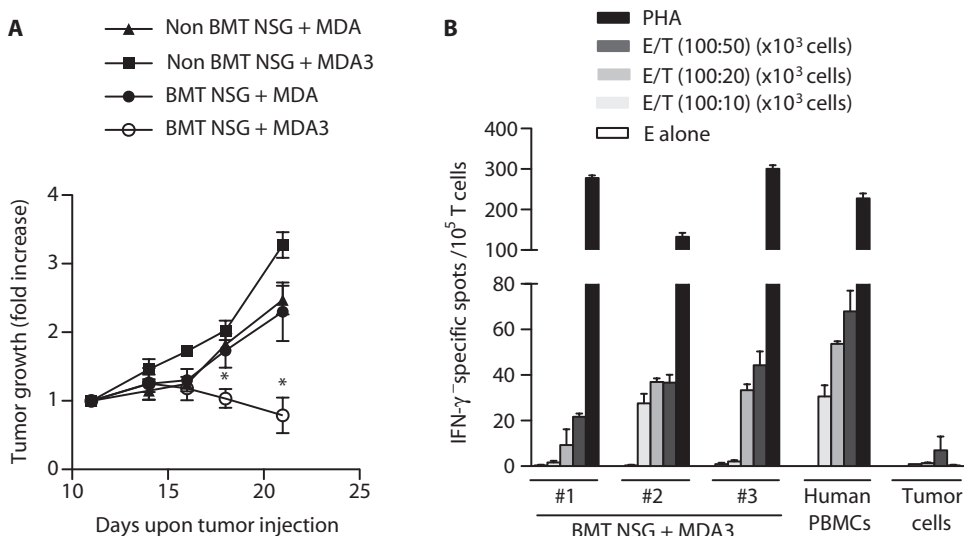


Fig. 4. Engineering the MDA-MB 231 breast cancer cell line to express human IL-7, IL-15, and GM-CSF improves human T cell functions and promotes effective tumor growth inhibition. (A) Tumor volume fold increase (over the tumor volume at day 11 upon tumor injection) in untransplanted NSG mice (non BMT NSG) injected with MDA ($n = 6$) or MDA3 ($n = 6$) cells, and NSG mice transplanted with human CD34⁺ cells (BMT NSG) and injected with MDA ($n = 3$) or MDA3 ($n = 7$) cells. * $P = 0.0293$ (day 18), $P = 0.0138$ (day 21), Student's t test. (B) Splenic T cells were purified from either human hematopoietic NSG mice or human healthy donors (PBMCs) and tested by IFN- γ enzyme-linked immunosorbent spot assay against the MDA-MB 231 tumor cell line at the indicated effector/target (E/T) ratio. PHA stimulation is used as a positive control. Tumor or T cells (E alone) alone are used as a negative control.

or MDA cells with similar efficiency as peripheral blood T cells from normal human donors (fig. S7D and Fig. 4B). Notably, tumor rejection was not accompanied by obvious signs of graft-versus-host disease in the mice, which appeared healthy when euthanized at the end of the experiments. Together, these results indicate development of a functional human immune system within the mouse that can reject an allogeneic human tumor while sparing the host mouse tissues.

Tumor inhibition in mice bearing human chimeric hematopoiesis engineered for IFN- α delivery by myelo-monocytes

We then investigated the cytokine dose response for tumor clearance by challenging human hematopoietic mice with MDA3 cells diluted 1:10 in the parental cells (termed MDA3.1). Although we still observed a substantial T cell and myeloid cell expansion in mice challenged with MDA3.1 cells as compared to MDA-injected mice, the increase in T cell number was lower than with undiluted MDA3 cells, and almost lacking for NK cells (Fig. 5A). MDA3.1 tumors were not rejected in *hTIE2*-GFP-mirT mice and grew as in MDA-injected control hosts (Fig. 5B).

We then asked whether genetic engineering of human hematopoiesis for tumor-targeted IFN- α delivery would enhance tumor rejection in this setting. When we compared *hTIE2*-GFP-mirT ($n = 7$) and *hTIE2*-IFN-mirT ($n = 8$) mice injected orthotopically with the MDA3.1 cells, we found that whereas T cell expansion was similar in both groups, there was marked inhibition of tumor growth only in *hTIE2*-IFN-mirT mice ($P = 0.0118$, day 21, Student's t test; Fig. 5B and fig. S8A). Similar results were obtained in a second independent experiment (fig. S8B). As observed in HS/PC-transplanted NSG mice challenged with MDA3 cells, there were no obvious signs of graft-versus-host disease in *hTIE2*-IFN-

mirT mice that rejected MDA3.1 tumors. Immunofluorescence staining showed that all MDA3.1 tumors were highly infiltrated by human T cells as compared to MDA controls (fig. S9A). Myeloid CD11c⁺ cells were also present, albeit to a lower extent, in all tumors. Notably, a fraction of these CD11c⁺ cells expressed DNCR1, which identifies a DC subset involved in antigen cross-presentation in response to type I IFN (fig. S9B) (6, 7). *IRF7* and *OAS1A* were slightly but significantly up-regulated in the tumors of *hTIE2*-IFN-mirT mice as compared to *hTIE2*-GFP-mirT mice (*IRF7* $P = 0.049$, *OAS1A* $P = 0.013$, Student's t test) (Fig. 5C). A trend toward up-regulation was also detected in the spleen.

To further prove that IFN- α expressed from the genetically engineered macrophages recruited within the tumor was sufficient to trigger an antitumor effect, we set up a tumor model based on mixing MDA3.1 cells with gene-modified monocytes followed by adoptive T cell transfer. We injected untransplanted NSG mice with MDA3.1 cells mixed or not with *hTIE2*-GFP-mirT- or *hTIE2*-IFN-mirT-transduced human blood monocytes, followed by intravenous delivery of T cells isogenic to

the monocytes (Fig. 5D). To efficiently transduce human blood monocytes, we preloaded the cells with Vpx-containing Simian immunodeficiency virus (SIV)-like particles before LV transduction (31), obtaining more than 60% cells expressing the GFP protein from the *hTIE2*-GFP-mirT construct (fig. S10A). When *hTIE2*-GFP-mirT monocytes were co-injected with MDA3.1 cells, tumor growth was accelerated, likely as a result of monocyte/macrophage-mediated promotion of tumor angiogenesis, as previously described (Fig. 5E) (11, 12). This tumor-promoting effect was abrogated when *hTIE2*-IFN-mirT-transduced monocytes were used. Moreover, tumors from the latter group showed increased infiltration by activated T cells (fig. S10, B and C). These findings suggest that forced IFN- α expression can reprogram the protumoral properties of the injected monocytes and boost the recruitment and activation of T cells within the tumor.

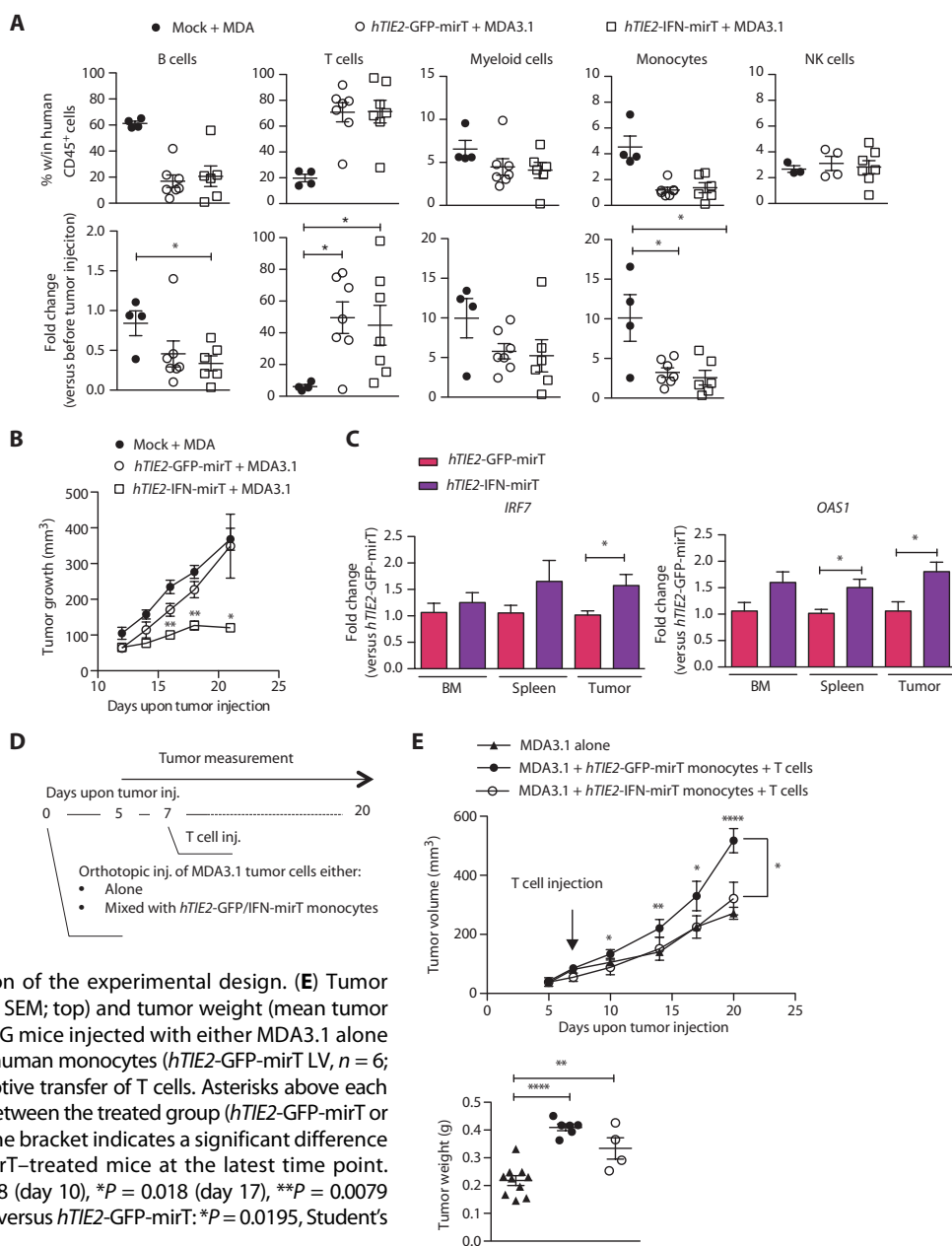
Overall, these results indicate that human IFN- α delivery by genetically engineered tumor-infiltrating macrophages induces a type I IFN response in the tumors that potentiates the deployment of antitumor immunity without obvious toxicity to the host.

Long-term hematopoietic repopulation sustained by murine HS/PCs engineered with a mouse mTie2-IFN transgene

The biological activity of IFN- α is strictly species-specific (32, 33). Thus, the xenotransplant model described above could only capture IFN- α effects on cells derived from the human graft and the tumor. To more stringently assess potential toxicity on multiple tissues (including bona fide HSC) and antitumor activity in settings that better represent immunocompetent hosts and multistep tumorigenesis, we performed additional studies using the mouse IFN- α transgene. We compared the previously described murine *mTie2*-IFN construct (13) with a homologous,

Fig. 5. Effective tumor growth inhibition in *hTIE2*-IFN-mirT NSG mice orthotopically injected with the engineered MDA3 breast cancer cell line.

(A) Percentages (top) and fold changes (bottom) of the absolute numbers of B cells, T cells, myeloid cells, monocytes, and NK cells present in the PB of MDA-injected mock ($n = 4$) and MDA3.1-injected *hTIE2*-GFP-mirT ($n = 6$) or *hTIE2*-IFN-mirT ($n = 7$) NSG mice. * $P = 0.0178$ (B cells), $P = 0.05$ (T cells mock versus *hTIE2*-IFN-mirT), $P = 0.0108$ (T cells mock versus *hTIE2*-GFP-mirT), $P = 0.0198$ (T cells mock versus *hTIE2*-GFP-mirT), $P = 0.0145$ (T cells mock versus *hTIE2*-GFP-mirT), Student's *t* test. Percentage is measured at 3 weeks upon tumor injection, and fold changes are calculated with respect to T_0 (before tumor injection). MDA, parental tumor cell line. MDA3.1, 1 to 10 dilution of MDA3 (that is, human IL-7-, IL-15-, and GM-CSF-expressing tumor cell line) into MDA tumor cells. (B) Tumor kinetic growth over time (mean tumor measurement \pm SEM) in MDA-injected mock ($n = 4$) or MDA3.1-injected *hTIE2*-GFP-mirT ($n = 6$) or *hTIE2*-IFN-mirT ($n = 8$) NSG mice. Statistical analysis was performed between *hTIE2*-GFP-mirT and *hTIE2*-IFN-mirT NSG mice. * $P = 0.0118$ (day 21), ** $P = 0.003$ (day 16), ** $P = 0.0013$ (day 18), Student's *t* test. (C) *IRF7* (left) and *OAS1* (right) expression (mean fold change over Ctrl organs \pm SEM) in tumors and organs from control (*hTIE2*-GFP-mirT, $n = 6$ to 7) and IFN-treated (*hTIE2*-IFN-mirT, $n = 6$ to 8) human hematohimic NSG mice, as measured by RT-qPCR. * $P = 0.049$ (*IRF7*), $P = 0.0184$ (*OAS1*, spleen), $P = 0.0133$ (*OAS1*, tumor), Student's *t* test. (D) Schematic representation of the experimental design. (E) Tumor growth kinetics (mean tumor measurement \pm SEM; top) and tumor weight (mean tumor weight \pm SEM; bottom) in untransplanted NSG mice injected with either MDA3.1 alone ($n = 10$) or MDA3.1 mixed with LV-transduced human monocytes (*hTIE2*-GFP-mirT LV, $n = 6$; *hTIE2*-IFN-mirT LV, $n = 4$), followed by the adoptive transfer of T cells. Asterisks above each measurement indicate significant differences between the treated group (*hTIE2*-GFP-mirT or *hTIE2*-IFN-mirT) and MDA3.1 alone, whereas the bracket indicates a significant difference between *hTIE2*-GFP-mirT- and *hTIE2*-IFN-mirT-treated mice at the latest time point. *hTIE2*-GFP-mirT versus MDA3.1 alone: * $P = 0.048$ (day 10), * $P = 0.018$ (day 17), ** $P = 0.0079$ (day 14), **** $P < 0.0001$ (day 21); *hTIE2*-IFN-mirT versus *hTIE2*-GFP-mirT: * $P = 0.0195$, Student's *t* test.



miR-126/130a-regulated construct (*mTie2*-IFN-mirT; Fig. 6A). Again, IFN- α expression was suppressed in endothelial cells by the mirT vector, and clonogenic assays did not reveal toxicity in hematopoietic progenitors with either of the constructs (fig. S11, A and B).

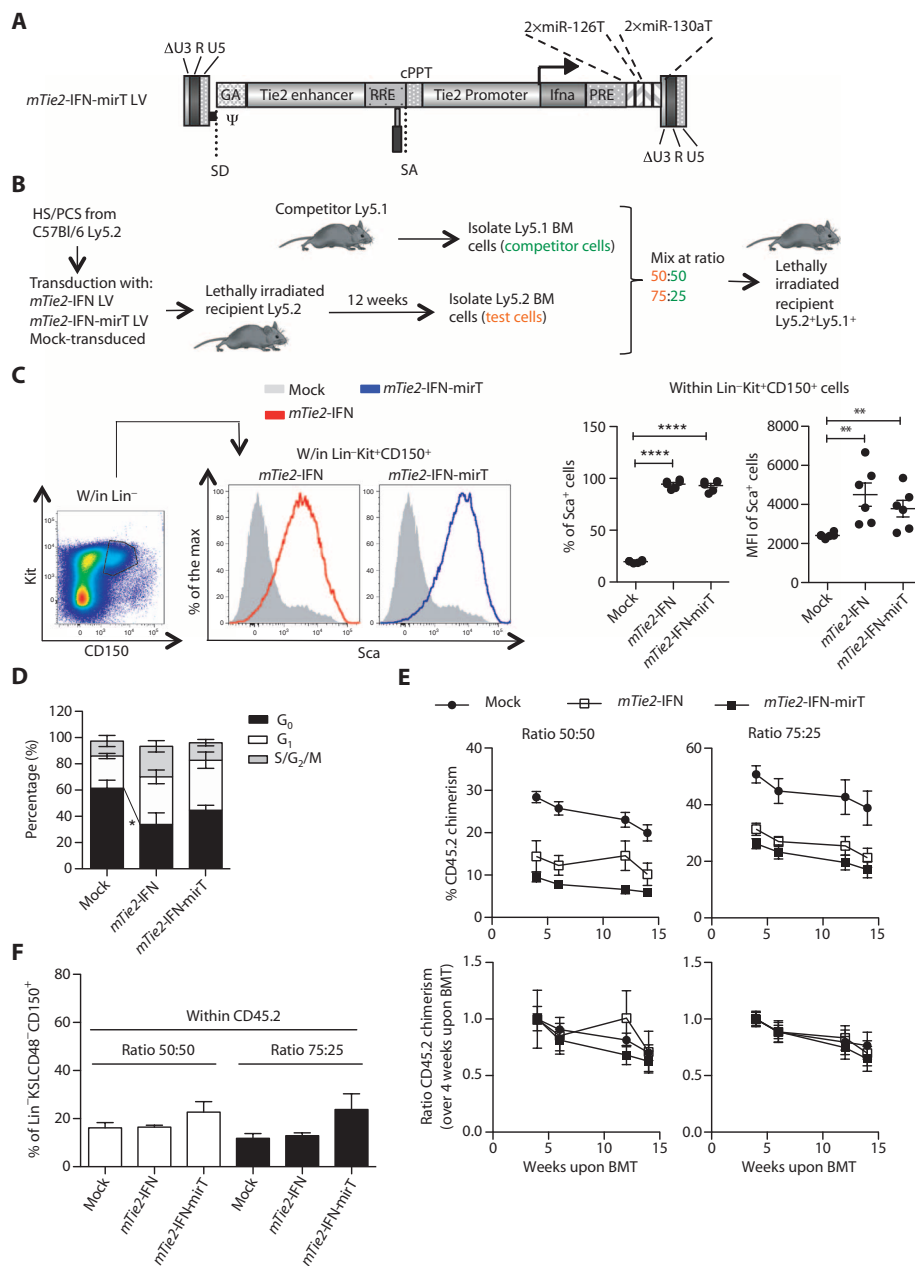
To stringently assess HSC toxicity, we transplanted C57Bl/6 Ly5.2 (CD45.2⁺) mice with *mTie2*-IFN LV- ($n = 12$), *mTie2*-IFN-mirT LV- ($n = 14$), or mock-transduced ($n = 16$) CD45.2⁺ HS/PCs (Fig. 6B). BM analysis 12 weeks after transplant showed up-regulation of the Sca1 molecule on Lineage⁻Kit⁺CD150⁺ cells in IFN-treated mice as compared to mock controls (Fig. 6C), with a trend toward lower up-regulation in *mTie2*-IFN-mirT versus *mTie2*-IFN mice [which had similar VCN per genome: 0.7 ± 0.1 (mean \pm SEM) and 0.5 ± 0.1 , respectively]. Cell cycle analysis performed on highly purified HSCs (Fig. 6D and fig.

S11, C and D) showed significantly fewer *mTie2*-IFN-transduced HSCs in G₀ phase as compared to mock (30 versus 60%; $n = 4$ pools of 3 mice for each group; $P = 0.0433$, Student's *t* test). The cell cycle status of HSCs derived from *mTie2*-IFN-mirT mice ($n = 4$ pools of 2 to 3 mice) did not significantly differ from that of control mice, suggesting that detargeting IFN- α expression from HS/PCs by miRNA regulation reduces nonphysiological activation of HSCs.

We then performed a secondary competitive transplant with competitor cells obtained from nontransplanted C57Bl/6 Ly5.1 (CD45.1⁺) mice at a 50:50 or 75:25 ratio, and assessed the ability of IFN-transduced (CD45.2⁺) HSCs to repopulate secondary recipients (Fig. 6B). Whereas BM cells from *mTie2*-IFN or *mTie2*-IFN-mirT mice contributed less efficiently to hematopoietic reconstitution of secondary recipients compared

Fig. 6. Reduced IFN-mediated activation of the HSC cell cycle in *mTie2*-IFN-miR mice and long-term multilineage repopulation of secondary recipients by IFN-treated BM cells in competitive settings.

(A) Schematic representation of the vector design. Abbreviations as in Fig. 1A. *Ilna*, murine IFN- α cDNA; miR-XT, target sequences for the indicated miRNAs. **(B)** Schematic representation of the experimental design. **(C)** Left: Representative plots showing Sca1 expression within the Lineage⁻Kit⁺CD150⁺ BM cells in *mTie2*-IFN (red open histogram) and *mTie2*-IFN-miR (blue open histogram) C57Bl/6 mice with respect to mock control mice (gray histograms) at 12 weeks upon primary transplant. Right: Percentage and MFI (mean \pm SEM) of Sca⁺ cells within Lineage⁻Kit⁺CD150⁺ cells in *mTie2*-IFN ($n = 6$), *mTie2*-IFN-miR ($n = 6$), and mock ($n = 6$) C57Bl/6 mice at 12 weeks upon primary transplant. **(D)** Cell cycle analysis (mean \pm SEM) performed on Lineage⁻Sca⁺Kit⁺CD48⁻CD150⁺ HSCs in mock ($n = 4$ pools of 3 mice), *mTie2*-IFN ($n = 3$ pools of 3 mice), and *mTie2*-IFN-miR ($n = 4$ pools of 2 to 3 mice) C57Bl/6 mice at 12 weeks upon transplant (primary transplant). **(E)** Top: Time course analysis of the percentage of CD45.2⁺ cells present in the PB of mock ($n = 6$), *mTie2*-IFN ($n = 5$ to 6), and *mTie2*-IFN-miR ($n = 8$ to 9) mice upon secondary transplant with a 50:50 or 75:25 ratio of CD45.2/CD45.1 cells. Bottom: Ratio of the percentages (mean \pm SEM) of CD45.2⁺ cells present in the PB at the indicated time point with respect to 4 weeks upon secondary transplant in mock ($n = 6$), *mTie2*-IFN ($n = 5$ to 6), and *mTie2*-IFN-miR ($n = 8$ to 9) mice. **(F)** Percentage (mean \pm SEM) of Lineage⁻Kit⁺Sca⁺CD48⁻CD150⁺ HSCs within the CD45.2⁺ cells present in the BM of mock ($n = 4$ to 6), *mTie2*-IFN ($n = 5$ to 6), and *mTie2*-IFN-miR ($n = 5$ to 7) mice at 15.5 weeks upon transplant with a 50:50 or 75:25 ratio of CD45.2/CD45.1 cells.



to BM cells from mock mice (Fig. 6E, top panel; $P = 0.0031$ and $P < 0.0001$, Student's t test, mock versus *mTie2*-IFN and *mTie2*-IFN-miR, respectively, at 4 weeks after BM transplant dose 50:50; $P = 0.0015$ and $P < 0.0001$, Student's t test, mock versus *mTie2*-IFN and *mTie2*-IFN-miR, respectively, at 4 weeks after BM transplant dose 75:25), this was likely due to lower HSC input or engraftment from the primary hosts and not to hematopoietic competition in the secondary hosts. Indeed, BM cells from *mTie2*-IFN or *mTie2*-IFN-miR mice sustained long-term (14 weeks after transplant) multilineage repopulation in secondary transplants. When we normalized post-engraftment levels for all experimental groups of CD45.2⁺ cells to their input levels, we found a similar contribution to the circulating cells over time (Fig. 6E, bottom panel) and a similar proportion of HSCs (defined as KSL CD48⁻CD150⁺ cells) among CD45.2⁺ BM cells at the end of the ex-

periment (Fig. 6F). Together, these data suggest that HSCs were fewer or engrafted less efficiently if harvested from the BM of *mTie2*-IFN or *mTie2*-IFN-miR mice, but were still able to sustain long-term repopulation of the mice. When we measured VCNs in the BM of secondary transplants at the end of the experiment and compared them to VCNs in the infused CD45.2⁺ cells harvested from primary transplants, we found that the fraction of IFN- α -transduced cells within the transplanted population decreased substantially upon secondary transplantation (fig. S11E).

Overall, these results indicate that the extent of exposure to transgenic IFN- α mediated by engineering hematopoiesis did not cause exhaustion of the HSC compartment and did not abrogate the potential to repopulate long-term secondary recipients. However, the lower contribution to engraftment by BM cells from *mTie2*-IFN mice,

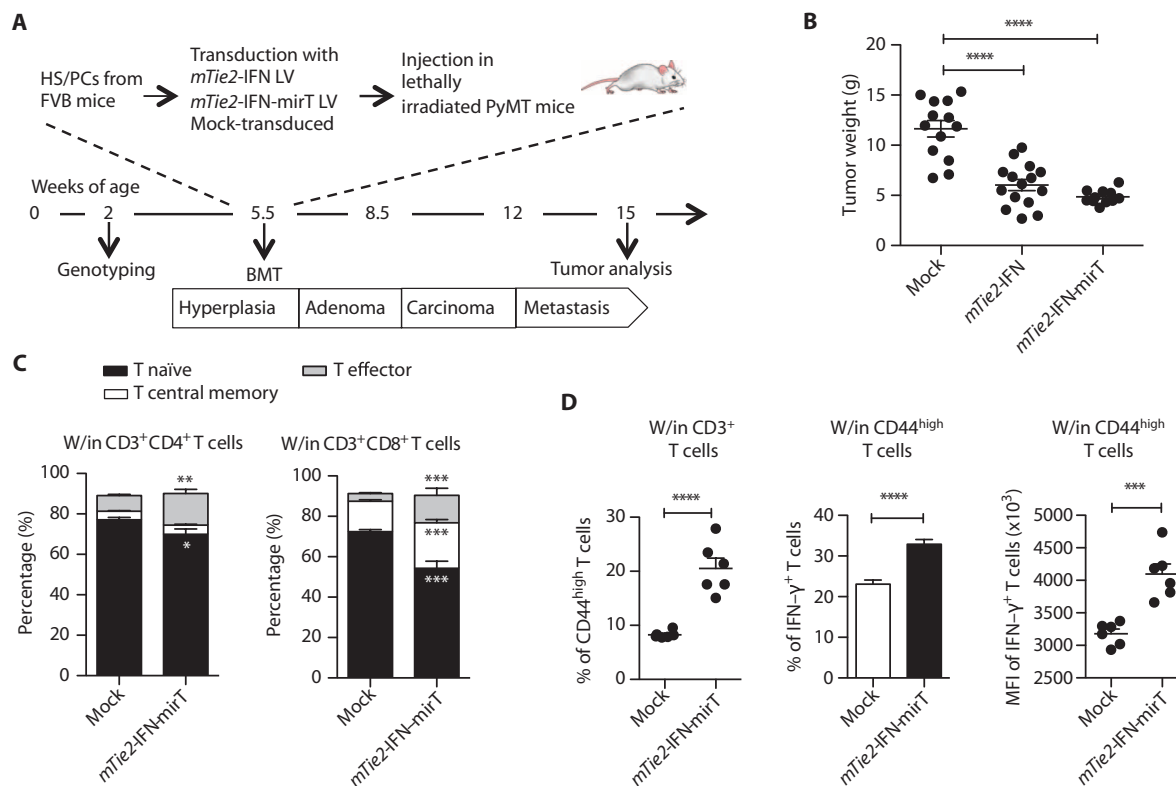


Fig. 7. Effective tumor growth inhibition in *mTie2*-IFN-mirT MMTV-PyMT mice. (A) Schematic representation of the experimental design. (B) Mammary tumor growth (mean tumor weight \pm SEM) at 15 weeks of age in control (mock; $n = 13$), *mTie2*-IFN ($n = 15$), and *mTie2*-IFN-mirT ($n = 11$) FVB/MMTV-PyMT mice. Two independent experiments are combined. **** $P < 0.0001$, Student's *t* test. (C) Percentages (mean \pm SEM) of T cell subpopulations within either CD4⁺ (left) or CD8⁺ (right) T cells in the spleen of 15-week-old

mock ($n = 6$) and *mTie2*-IFN-mirT ($n = 6$) FVB/MMTV-PyMT mice. Within CD3⁺CD4⁺ T cells: * $P = 0.0355$, ** $P = 0.0012$; within CD3⁺CD8⁺ T cells: *** $P = 0.0005$ (naïve), $P = 0.0008$ (central memory), $P = 0.0009$ (effector memory); Student's *t* test. (D) Percentage (mean \pm SEM) of effector CD44^{high} T cells (left) and percentage (center) and mean MFI (right) (mean \pm SEM) of IFN- γ ⁺ cells within CD44^{high} T cells in 15-week-old mock ($n = 6$) and *mTie2*-IFN-mirT ($n = 6$) FVB/MMTV-PyMT mice. *** $P = 0.0004$, **** $P < 0.0001$, Student's *t* test.

together with the decreasing proportion of engineered cells upon serial transplantation, suggests the occurrence of a progressive loss of the engineered HSCs. This may provide a built-in safeguard mechanism against permanent modification of hematopoiesis. This safety feature appeared to remain functional even when deploying the miRNA-regulated vector.

Inhibition of primary mammary tumors in MMTV-PyMT transgenic mice with *mTie2*-IFN-engineered hematopoiesis

We investigated the antitumor activity of the new *mTie2*-IFN-mirT LV platform in an oncogene-driven mouse model of mammary carcinogenesis. We transplanted 5.5-week-old transgenic MMTV-PyMT mice with HS/PCs either transduced with the *mTie2*-IFN ($n = 15$) or *mTie2*-IFN-mirT ($n = 11$) LVs or mock-transduced ($n = 13$) (Fig. 7A). At 15 weeks of age, we observed significant inhibition of the multifocal and rapidly growing tumors ($P < 0.0001$, Student's *t* test), typically observed in this model, in both IFN vector groups (Fig. 7B). Notably, tumor inhibition was achieved even with a low chimerism of gene-modified cells [VCN: 0.14 ± 0.05 (mean \pm SEM) in BM cells of *mTie2*-IFN-mirT mice; 1.1 ± 0.2 in BM cells of *mTie2*-IFN mice]. Although there were no differences in the total number of splenic CD3⁺, CD4⁺, and CD8⁺ T cells between the two groups (fig. S12A), we found an increased proportion of effector CD4⁺ and CD8⁺ T cells and central

memory CD8⁺ T cells in *mTie2*-IFN-mirT mice (Fig. 7C and fig. S12B). Splenocytes of *mTie2*-IFN-mirT mice after ex vivo stimulation displayed a higher percentage of CD44^{high} effector T cells ($P < 0.0001$, Student's *t* test), which produced higher IFN- γ levels compared with control cells (Fig. 7D and fig. S12C). These data suggest enhanced immune cell activation in tumor-bearing mice with *mTie2*-IFN-engineered hematopoiesis. BM analysis showed some signs of activation of the HSC compartment, which were alleviated by the mirT construct, as described above for C57Bl/6 mice (fig. S13, A and B).

Inhibition of experimental lung metastases in mice bearing *mTie2*-IFN-engineered hematopoiesis

To test the ability of *mTie2*-IFN-engineered hematopoiesis to directly suppress the growth of late-stage carcinoma cells, we injected PyMT cells derived from advanced metastatic primary tumors into the tail vein of wild-type FVB mice either transplanted with mock- or *mTie2*-IFN-mirT-transduced HS/PCs (Fig. 8A). All mock mice had metastatic outgrowth in the lung (Fig. 8B), with multiple large metastases ($n = 6$ mice; average total metastatic area, 12.6 mm^2 ; 29 to 54 sections examined per mouse). *mTie2*-IFN-mirT mice showed a highly significant reduction in the size of the metastatic foci and a trend toward a reduced number of metastases ($n = 6$; average total metastatic area, 2.3 mm^2 ; 22 to 43 sections examined per mouse). The total tumor area

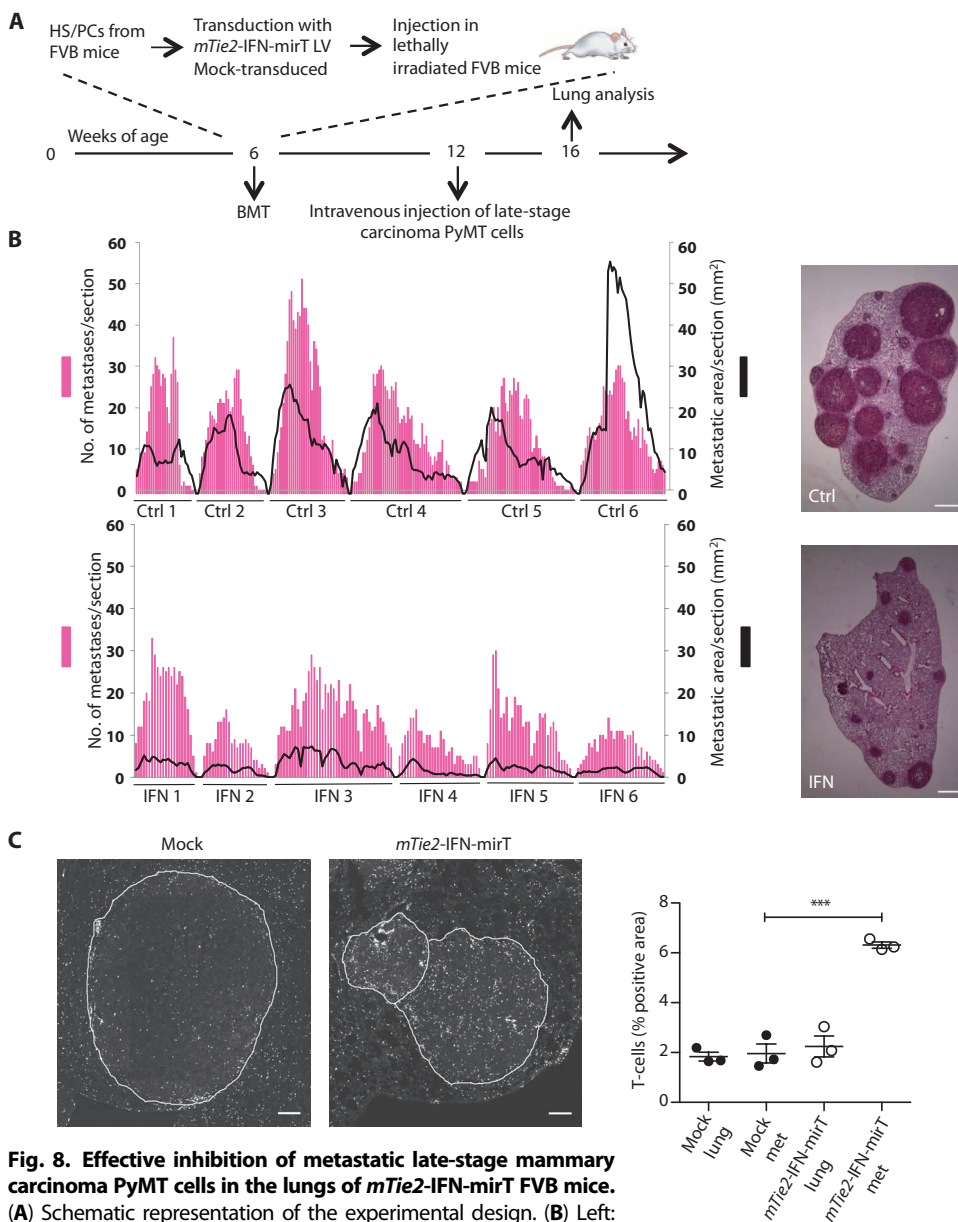


Fig. 8. Effective inhibition of metastatic late-stage mammary carcinoma PyMT cells in the lungs of *mTie2*-IFN-mirT FVB mice.

(A) Schematic representation of the experimental design. (B) Left: Number of metastatic foci (purple bars) and total metastatic area (black line) in single serial sections (individual bars) of the entire left lung of each of the control (Ctrl; $n = 6$) and *mTie2*-IFN-mirT (IFN; $n = 6$) FVB mice. Mice were analyzed 4 weeks after the intravenous injection of metastatic late-stage carcinoma PyMT cells. Right: Hematoxylin and eosin staining of representative lung sections of control (Ctrl) and *mTie2*-IFN-mirT-transplanted (IFN) FVB mice treated as described above. Scale bar, 1 mm. (C) Representative confocal images (left) and quantitative analysis (right; mean \pm SEM) of the T cell immunostaining on lung sections in the normal lung parenchyma (lung) or in the metastatic nodules (met) of mock (full dots; $n = 3$) and *mTie2*-IFN-mirT (open dots; $n = 3$) mice. Dashed lines indicate tumor margin. Scale bar, 150 μ m. *** $P = 0.0004$, Student's t test.

was, on average, more than fivefold greater in control versus *mTie2*-IFN-mirT mice ($P = 0.0022$, Mann-Whitney test). These results demonstrate a direct antitumor effect of the engineered hematopoietic cells on experimental lung metastases. The observed effects were obtained at low chimerism of gene-modified cells (VCN: 0.34 ± 0.1 , mean \pm SEM).

We then measured the extent of T cell infiltration in the metastatic nodules of *mTie2*-IFN-mirT and mock mice (Fig. 8C) and found that it was significantly higher in the former ($P = 0.0004$, Student's t test), whereas no difference was found in the surrounding lung parenchyma. Notably, T cells from control mice tended to cluster at the metastasis margins but did not infiltrate the tumor mass. Together, these results indicate that engineering hematopoiesis for transgenic IFN- α expression in monocytes/macrophages enhances the recruitment and activation of immune effector cells, thus leading to effective inhibition of metastatic growth of breast cancer cells.

DISCUSSION

We here provide comprehensive preclinical data supporting the feasibility, safety, and therapeutic efficacy of genetically engineering human HS/PCs for tumor-targeted IFN- α delivery by monocytes/macrophages. We developed an LV that switches on transgene expression in the myeloid progeny of transduced HS/PCs and allows high transgene expression in mature, tumor-infiltrating macrophages. This was achieved by using a combination of transcriptional targeting to the monocyte lineage, mediated by human *TIE2* enhancer/promoter sequences, and posttranscriptional detargeting from early progenitors, mediated by endogenous miR-126 and miR-130a (26). Because of the lack of cross-reactivity between human IFN- $\alpha 2$ and mouse tissues (32, 33), we performed our studies using the human or mouse IFN- α transgene in human hematochimeric mice challenged with tumor xenografts or in mice spontaneously developing breast cancer transplanted with engineered murine HS/PCs, respectively. These approaches comprehensively interrogate the therapeutic and potential adverse interactions between the transgene, the tumor, and the host.

We assessed the specificity of our vector by analyzing reporter GFP expression in the reconstituted hematopoiesis of transplanted mice and by tracking IFN-induced responses in the host tissues, which provides a sensitive readout for biologically relevant IFN- α expression. Preferential targeting of myeloid- versus lymphoid-lineage cells was shown by the differential frequency of reporter-positive cells and the mean expression level of the reporter in the two hematopoietic

compartments. miRNA regulation effectively suppressed transgene expression in HS/PCs. Furthermore, IFN-responsive genes were significantly up-regulated mostly at the tumor site and less markedly in the spleen and BM of transplanted mice. These data highlight the targeting specificity achieved by our genetic platform, particularly if one considers the differential contribution of hematopoietic cells to tissues in NSG mice, which is minimal in the tumor and nearly exhaustive in hematolymphoid tissues. The basis for such specificity is likely to be the up-regulation of the *TIE2* promoter in differentiated macrophages, a process that occurs preferentially in tumor-infiltrating macrophages among other tissue-resident macrophages (34). A residual level of transgenic IFN- α expression is expected in the spleen and BM of transplanted mice because of the large pool of monocytes/macrophages found in these organs (35). In fact, we observed Sca1 up-regulation in progenitors and increased cell cycle progression of HSCs in the BM of *mTie2*-IFN mice, two previously reported signs of IFN- α exposure (19, 24). These phenotypes were alleviated but not abrogated by inclusion of mirT sequences in the LV, suggesting that differentiated TIE2⁺ myeloid cells could function as a paracrine source of IFN- α . HSCs harvested from the BM of *mTie2*-IFN (with or without mirT) mice did not exhaust in competitive serial transplantation experiments. This outcome is reassuring in view of previous studies that reported competitive disadvantage of HSCs chronically exposed to exogenous IFN- α or made hypersensitive to IFN- α signaling by *Irf2*, *Adar*, or *Irgm1* knockout (19, 24, 36, 37). The lack of HSC exhaustion in our study implies that the overall level of IFN- α expression in the BM of transplanted *mTie2*-IFN mice is limited by the specific LV design. We did observe, however, counterselection of the genetically modified HSCs (*mTie2*-IFN LV with or without mirT) in serially transplanted BM cells. The latter finding may be explained postulating that exposure to IFN- α locally varies within the BM and may cause selective exposure of the engineered HSCs to IFN- α via juxtacrine secretion by their nearby differentiated myeloid progeny. This may lead to increased activation of the transduced HSCs and impaired engraftment upon serial transplant. This scenario would make our HSC engineering strategy self-limiting in the long term, providing an added safety feature from the standpoint of clinical testing. Dose escalation studies of *hTIE2*-IFN-mirT gene transfer performed on human HS/PCs from clinically relevant sources, such as BM or mobilized peripheral blood, are required to further address potential hematopoietic toxicity and the in vivo persistence of transduced HS/PCs.

The antitumor efficacy of our strategy was demonstrated in a human hematochimeric mouse model permissive to the development of cell-mediated immune responses. Human cytokines have been administered or expressed in NSG mice by different approaches to overcome the limited myeloid, NK, and T cell reconstitution by transplanted human HS/PCs (30). We engineered the human breast tumor cell line (MDA-MB 231) to release, in addition to high levels of G-CSF, human IL-7, IL-15, and GM-CSF. By challenging human hematochimeric NSG mice with these tumor cells, we observed tumor cell rejection, likely mediated by alloreactive human T cells developed within the mouse thymus, and thus tolerant to the host tissues, and by the expanded human NK cells (fig. S14). Because tumor cells were rapidly cleared in these mice, the exogenous source of cytokines was rapidly exhausted as well. It is likely, however, that the expanded innate and adaptive immune cell populations triggered by the initial tumor implant become themselves a source of some required cytokine. By lowering the dose of exogenous cytokines released by the tumor implant, we could demonstrate the enhanced capacity of human hematopoiesis

engineered for targeted delivery of IFN- α to mount an effective immune response leading to tumor rejection, which was associated with activation of a type I IFN response in the tumor, without causing obvious graft-versus-host disease. Several mechanisms may underlie the IFN-enhanced antitumor response. The proangiogenic activity of tumor-associated macrophages may be directly counteracted by the engineered expression of IFN- α , as shown by mixing the tumor cell challenge with blood monocytes transduced with the *hTIE2*-IFN-mirT or control vector. DCs recruited to the tumor, including the DNGR1-expressing subset, may be stimulated by paracrine or autocrine transgenic IFN- α expression (fig. S15) to enhance costimulation and cross-presentation of tumor antigens, resulting in more effective induction of T cell responses (6, 7). Indeed, human T cells highly infiltrate the tumor and likely mediate its rejection. NK cells, despite being poorly expanded by the lower cytokine doses found in these settings, are also activated by IFN and may contribute to tumor inhibition.

Parallel studies in the murine PyMT breast cancer model established that our strategy can efficiently inhibit tumor growth, progression, and experimental metastases in an autologous/syngeneic setting, primarily by enhancing the generation of memory and effector T cells and their recruitment to the neoplastic lesions. It will be interesting to identify the antigens targeted by tumor-infiltrating effector T cells in these settings, which might uncover tumor-associated antigens of possible clinical relevance. Because in this model the IFN- α transgene and the host belong to the same species, a direct antiangiogenic effect of IFN- α on tumor endothelial cells may contribute to the antitumor response, consistent with our previous studies (13). This therapeutic mechanism would likely be operational in clinical settings.

Recent studies have implicated IFN- α signaling to host immune cells as a metastasis suppressor mechanism, and shown that metastatic breast cancer cells from human patients preferentially down-regulate *IRF7* target genes (38). These findings strengthen the rationale for clinical translation of our strategy. Nevertheless, it remains to be seen whether genetic engineering of human hematopoiesis for IFN- α expression in NSG mice would also be effective against advanced tumors or spontaneous metastases.

Our data could revive interest in testing high-dose chemotherapy followed by autologous HSC transplantation in advanced breast cancer patients (39, 40). Because we showed antitumor efficacy even at low chimerism of transduced cells, we envisage genetic modification of only a fraction of HSCs to limit potential IFN- α exposure and toxicity. Moreover, our strategy could be tested in other malignancies for which autologous HSC transplantation is currently adopted as a therapeutic regimen, such as lymphoma and multiple myeloma, for which previous studies have shown some efficacy of IFN- α administration (41–43). If proved safe and effective in humans, our strategy could also be combined with other immunotherapeutic approaches to best exploit the biological weapons of immunity in the unrelenting fight against cancer.

MATERIALS AND METHODS

Study design

All mice were randomized into different HSC transplantation groups. On the basis of a standard backward sample size calculation, in each experiment, we transplanted at least eight mice per condition and performed at least two independent experiments to obtain a sufficient

number of mice to have a statistical power of 0.8 with a level of significance of 0.05 and an estimated effect size of 0.8. Often, more than eight mice per condition were transplanted to compensate for the possible loss of mice due to the BM transplantation procedure. The outcomes of the following analyses were blindly assessed: experimental PyMT lung metastasis quantification, T cell infiltrate quantification on lung sections with experimental PyMT lung metastasis, and human tumor growth measurements.

BM transplantation in NSG mice and orthotopic injection of human breast cancer cells

Human cord blood–derived CD34⁺ cells (purchased from Lonza, 2C-101) were prestimulated and transduced with the indicated LV as described in Supplementary Materials and Methods. After transduction, 3×10^5 or 1.5×10^5 cells were infused into the tail vein of sublethally irradiated 10-week-old NSG mice. The parental MDA and the transduced MDA3 human mammary carcinoma cells (see Supplementary Materials and Methods) were implanted orthotopically (4×10^6 cells in 50 μ l) in the mammary fat pad of 23-week-old NSG females 13 weeks upon transplantation of transduced or mock-transduced human CD34⁺ cells.

BM transplantation in FVB, FVB/MMTV-PyMT, and C57Bl/6 mice

Lineage-negative cells enriched in HS/PCs were isolated from total BM of 6-week-old FVB or C57Bl/6 Ly45.2 and transduced with the indicated LV as described in Supplementary Materials and Methods. After transduction, cells were infused into the tail vein of lethally irradiated 6-week-old FVB and C57Bl/6 Ly45.2 females or 5.5-week-old FVB/MMTV-PyMT females. Secondary competitive BM transplantation in C57Bl/6 Ly45.1/Ly45.2 mice was performed as described in Supplementary Materials and Methods.

Experimental MMTV-PyMT metastases

Primary FVB/MMTV-PyMT metastatic tumor cells were obtained from late-stage tumors of 16-week-old FVB/MMTV-PyMT mice as described in Supplementary Materials and Methods, and 10^5 tumor cells were intravenously injected into 13-week-old FVB females 7 weeks upon transplantation of transduced or mock-transduced HS/PCs.

Statistical analysis

In all studies, values are expressed as means \pm SD or SEM, as indicated. Statistical analyses were performed by unpaired Student's *t* test or Mann-Whitney test, as indicated. Percentages were converted into log odds for statistical analysis. Differences were considered statistically significant at $P < 0.05$.

SUPPLEMENTARY MATERIALS

www.sciencetranslationalmedicine.org/cgi/content/full/6/217/217ra3/DC1

Materials and Methods

Fig. S1. Targeted transgene expression in human endothelial cells by an LV exploiting the human *TIE2* gene regulatory sequences.

Fig. S2. Hematopoietic reconstitution by transplanted cord blood–derived CD34⁺ human cells in the peripheral blood of NSG mice.

Fig. S3. Hematopoietic reconstitution by transplanted cord blood–derived CD34⁺ human cells in the BM of NSG mice.

Fig. S4. Effective in vitro suppression of human IFN- α expression in miR-126–expressing cells transduced with the *hTIE2*-IFN-miR-T and absence of overt toxicity of *hTIE2*-IFN-miR-T-transduced cord blood–derived human CD34⁺ cells.

Fig. S5. Human hematopoietic cells infiltrate MDA-MB 231 tumors grown in NSG mice.

Fig. S6. MDA3 tumor cells.

Fig. S7. T, myeloid, and NK cell expansion in human hematohimic NSG mice challenged with MDA3 cells.

Fig. S8. Tumor growth inhibition in MDA3.1-injected mice upon IFN- α delivery.

Fig. S9. Effective recruitment of innate and adaptive immune cells in MDA3.1 tumors grown in NSG mice.

Fig. S10. Adoptive transfer of human T cells in untransplanted NSG mice injected with MDA3.1 tumors mixed with *hTIE2*-GFP-miR- or *hTIE2*-IFN-miR-T-transduced human monocytes.

Fig. S11. Effective in vitro suppression of murine IFN- α expression in miR-126–expressing cells transduced with *mTie2*-IFN-miR-T LV and protection from IFN-mediated activation of HSC cell cycle in *mTie2*-IFN-miR-T-transduced HSCs.

Fig. S12. Splenic T cells in IFN-treated mice.

Fig. S13. Reduced HSC activation and Sca1 up-regulation upon engineering HS/PCs with the miRNA-regulated *mTie2*-IFN- α vector.

Fig. S14. NK and T cells contribute to mediate tumor growth inhibition in MDA3-injected human hematohimic NSG mice.

Fig. S15. Characterization of murine Tie2 promoter activity in the spleen of transgenic Tie2-GFP mice.

Table S1. List of anti-human antibodies used for flow cytometry.

Table S2. List of anti-murine antibodies used for flow cytometry.

References (44–47)

REFERENCES AND NOTES

- M. D. Vesely, M. H. Kershaw, R. D. Schreiber, M. J. Smyth, Natural innate and adaptive immunity to cancer. *Annu. Rev. Immunol.* **29**, 235–271 (2011).
- R. R. Jenq, M. R. van den Brink, Allogeneic haematopoietic stem cell transplantation: Individualized stem cell and immune therapy of cancer. *Nat. Rev. Cancer* **10**, 213–221 (2010).
- S. L. Topalian, G. J. Weiner, D. M. Pardoll, Cancer immunotherapy comes of age. *J. Clin. Oncol.* **29**, 4828–4836 (2011).
- D. Lindau, P. Gielen, M. Kroesen, P. Wesseling, G. J. Adema, The immunosuppressive tumour network: Myeloid-derived suppressor cells, regulatory T cells and natural killer T cells. *Immunology* **138**, 105–115 (2013).
- G. P. Dunn, A. T. Bruce, K. C. Sheehan, V. Shankaran, R. Uppaluri, J. D. Bui, M. S. Diamond, C. M. Koebel, C. Arthur, J. M. White, R. D. Schreiber, A critical function for type I interferons in cancer immunoeediting. *Nat. Immunol.* **6**, 722–729 (2005).
- M. B. Fuentes, A. K. Kacha, J. Kline, S. R. Woo, D. M. Kranz, K. M. Murphy, T. F. Gajewski, Host type I IFN signals are required for antitumor CD8⁺ T cell responses through CD8 α ⁺ dendritic cells. *J. Exp. Med.* **208**, 2005–2016 (2011).
- M. S. Diamond, M. Kinder, H. Matsushita, M. Mashayekhi, G. P. Dunn, J. M. Archambault, H. Lee, C. D. Arthur, J. M. White, U. Kalinke, K. M. Murphy, R. D. Schreiber, Type I interferon is selectively required by dendritic cells for immune rejection of tumors. *J. Exp. Med.* **208**, 1989–2003 (2011).
- S. Hervas-Stubbis, J. L. Perez-Gracia, A. Rouzaut, M. F. Sanmamed, A. Le Bon, I. Melero, Direct effects of type I interferons on cells of the immune system. *Clin. Cancer Res.* **17**, 2619–2627 (2011).
- B. X. Wang, R. Rahbar, E. N. Fish, Interferon: Current status and future prospects in cancer therapy. *J. Interferon Cytokine Res.* **31**, 545–552 (2011).
- S. Anguille, E. Lion, Y. Willemen, V. F. Van Tendeloo, Z. N. Berneman, E. L. Smits, Interferon- α in acute myeloid leukemia: An old drug revisited. *Leukemia* **25**, 739–748 (2011).
- M. De Palma, M. A. Venneri, R. Galli, L. Sergi Sergi, L. S. Politi, M. Sampaolesi, L. Naldini, Tie2 identifies a hematopoietic lineage of proangiogenic monocytes required for tumor vessel formation and a mesenchymal population of pericyte progenitors. *Cancer Cell* **8**, 211–226 (2005).
- M. A. Venneri, M. De Palma, M. Ponzoni, F. Pucci, C. Scielzo, E. Zonari, R. Mazzeri, C. Doglioni, L. Naldini, Identification of proangiogenic TIE2-expressing monocytes (TEMs) in human peripheral blood and cancer. *Blood* **109**, 5276–5285 (2007).
- M. De Palma, R. Mazzeri, L. S. Politi, F. Pucci, E. Zonari, G. Sitia, S. Mazzoleni, D. Moi, M. A. Venneri, S. Indraccolo, A. Falini, L. G. Guidotti, R. Galli, L. Naldini, Tumor-targeted interferon- α delivery by Tie2-expressing monocytes inhibits tumor growth and metastasis. *Cancer Cell* **14**, 299–311 (2008).
- N. Cartier, S. Hacein-Bey-Abina, C. C. Bartholomae, G. Veres, M. Schmidt, I. Kutschera, M. Vidaud, U. Abel, L. Dal-Cortivo, L. Caccavelli, N. Mahlaoui, V. Kiermer, D. Mittelstaedt, C. Bellesme, N. Lahlou, F. Lefrère, S. Blanche, M. Audit, E. Payen, P. Leboulch, B. l'Homme, P. Bougnères, C. Von Kalle, A. Fischer, M. Cavazzana-Calvo, P. Aubourg, Hematopoietic stem cell gene therapy with a lentiviral vector in X-linked adrenoleukodystrophy. *Science* **326**, 818–823 (2009).
- M. Cavazzana-Calvo, E. Payen, O. Negre, G. Wang, K. Hehir, F. Fusil, J. Down, M. Denaro, T. Brady, K. Westerman, R. Cavalleco, B. Gillet-Legrand, L. Caccavelli, R. Sgarra, L. Maouche-Chretien,

- F. Bernaudin, R. Giro, R. Dorazio, G. J. Mulder, A. Polack, A. Bank, J. Soulier, J. Larghero, N. Kabbara, B. Dalle, B. Gourmel, G. Socie, S. Chretien, N. Cartier, P. Aubourg, A. Fischer, K. Cornetta, F. Galacteros, Y. Beuzard, E. Gluckman, F. Bushman, S. Hacin-Bey-Abina, P. Leboulch, Transfusion independence and HMG2 activation after gene therapy of human β -thalassaemia. *Nature* **467**, 318–322 (2010).
16. A. Biffi, E. Montini, L. Lorioli, M. Cesani, F. Fumagalli, T. Plati, C. Baldoli, S. Martino, A. Calabria, S. Canale, F. Benedicenti, G. Vallanti, L. Biasco, S. Leo, N. Kabbara, G. Zanetti, W. B. Rizzo, N. A. Mehta, M. P. Cicalese, M. Casiraghi, J. J. Boelens, U. Del Carro, D. J. Dow, M. Schmidt, A. Assanelli, V. Neduva, C. Di Serio, E. Stupka, J. Gardner, C. von Kalle, C. Bordignon, F. Ciceri, A. Rovelli, M. G. Roncarolo, A. Aiuti, M. Sessa, L. Naldini, Lentiviral hematopoietic stem cell gene therapy benefits metachromatic leukodystrophy. *Science* **341**, 1233158 (2013).
17. A. Aiuti, L. Biasco, S. Scaramuzza, F. Ferrua, M. P. Cicalese, C. Baricordi, F. Dionisio, A. Calabria, S. Giannelli, M. C. Castiello, M. Bosticardo, Z. Waibler, U. Assanelli, M. Casiraghi, S. Di Nunzio, L. Callegaro, C. Benati, P. Rizzardi, D. Pellini, C. Di Serio, M. Schmidt, C. Von Kalle, J. Gardner, N. Mehta, V. Neduva, D. J. Dow, A. Galy, R. Miniero, A. Finocchi, A. Metin, P. P. Banerjee, J. S. Orange, S. Galimberti, M. G. Valsecchi, A. Biffi, E. Montini, A. Villa, F. Ciceri, M. G. Roncarolo, L. Naldini, Lentiviral hematopoietic stem cell gene therapy in patients with Wiskott-Aldrich syndrome. *Science* **341**, 1233151 (2013).
18. J. J. Kiladjan, C. Chomienne, P. Fenaux, Interferon- α therapy in bcr-abl-negative myeloid-proliferative neoplasms. *Leukemia* **22**, 1990–1998 (2008).
19. M. A. Essers, S. Offner, W. E. Blanco-Bose, Z. Waibler, U. Kalinke, M. A. Duchosal, A. Trumpp, IFN α activates dormant haematopoietic stem cells in vivo. *Nature* **458**, 904–908 (2009).
20. M. De Palma, M. A. Venneri, L. Naldini, In vivo targeting of tumor endothelial cells by systemic delivery of lentiviral vectors. *Hum. Gene Ther.* **14**, 1193–1206 (2003).
21. L. D. Shultz, B. L. Lyons, L. M. Burzenski, B. Gott, X. Chen, S. Chaleff, M. Kotb, S. D. Gillies, M. King, J. Mangada, D. L. Greiner, R. Handgretinger, Human lymphoid and myeloid cell development in NOD/LtSz-scid IL2R γ ^{null} mice engrafted with mobilized human hemopoietic stem cells. *J. Immunol.* **174**, 6477–6489 (2005).
22. F. Ishikawa, M. Yasukawa, B. Lyons, S. Yoshida, T. Miyamoto, G. Yoshimoto, T. Watanabe, K. Akashi, L. D. Shultz, M. Harada, Development of functional human blood and immune systems in NOD/SCID/IL2 receptor γ chain^{null} mice. *Blood* **106**, 1565–1573 (2005).
23. F. Arai, A. Hirao, M. Ohmura, H. Sato, S. Matsuoka, K. Takubo, K. Ito, G. Y. Koh, T. Suda, Tie2/angiopoietin-1 signaling regulates hematopoietic stem cell quiescence in the bone marrow niche. *Cell* **118**, 149–161 (2004).
24. T. Sato, N. Onai, H. Yoshihara, F. Arai, T. Suda, T. Ohteki, Interferon regulatory factor-2 protects quiescent hematopoietic stem cells from type I interferon-dependent exhaustion. *Nat. Med.* **15**, 696–700 (2009).
25. E. R. Lechman, B. Gentner, P. van Galen, A. Giustacchini, M. Saini, F. E. Boccalatte, H. Hiramatsu, U. Restuccia, A. Bachi, V. Voisin, G. D. Bader, J. E. Dick, L. Naldini, Attenuation of miR-126 activity expands HSC in vivo without exhaustion. *Cell Stem Cell* **11**, 799–811 (2012).
26. B. Gentner, I. Visigalli, H. Hiramatsu, E. Lechman, S. Ungari, A. Giustacchini, G. Schira, M. Amendola, A. Quattrini, S. Martino, A. Orlacchio, J. E. Dick, A. Biffi, L. Naldini, Identification of hematopoietic stem cell-specific miRNAs enables gene therapy of globoid cell leukodystrophy. *Sci. Transl. Med.* **2**, 58ra84 (2010).
27. S. Wang, A. B. Aurora, B. A. Johnson, X. Qi, J. McAnally, J. A. Hill, J. A. Richardson, R. Bassel-Duby, E. N. Olson, The endothelial-specific microRNA miR-126 governs vascular integrity and angiogenesis. *Dev. Cell* **15**, 261–271 (2008).
28. D. Metcalf, Hematopoietic cytokines. *Blood* **111**, 485–491 (2008).
29. M. Kowanetz, X. Wu, J. Lee, M. Tan, T. Hagenbeek, X. Qu, L. Yu, J. Ross, N. Korsisaari, T. Cao, H. Bou-Reslan, D. Kallop, R. Weimer, M. J. Ludlam, J. S. Kaminker, Z. Modrusan, N. van Bruggen, F. V. Peale, R. Carano, Y. G. Meng, N. Ferrara, Granulocyte-colony stimulating factor promotes lung metastasis through mobilization of Ly6G+Ly6C+ granulocytes. *Proc. Natl. Acad. Sci. U.S.A.* **107**, 21248–21255 (2010).
30. A. Rongvaux, H. Takizawa, T. Strowig, T. Willinger, E. E. Eynon, R. A. Flavell, M. G. Manz, Human hemato-lymphoid system mice: Current use and future potential for medicine. *Annu. Rev. Immunol.* **31**, 635–674 (2013).
31. G. Berger, S. Durand, C. Goujon, X. N. Nguyen, S. Cordeil, J. L. Darlix, A. Cimarelli, A simple, versatile and efficient method to genetically modify human monocyte-derived dendritic cells with HIV-1-derived lentiviral vectors. *Nat. Protoc.* **6**, 806–816 (2011).
32. M. Streuli, A. Hall, W. Boll, W. E. Stewart II, S. Nagata, C. Weissmann, Target cell specificity of two species of human interferon- α produced in *Escherichia coli* and of hybrid molecules derived from them. *Proc. Natl. Acad. Sci. U.S.A.* **78**, 2848–2852 (1981).
33. H. Weber, D. Valenzuela, G. Lujber, M. Gubler, C. Weissmann, Single amino acid changes that render human IFN- α 2 biologically active on mouse cells. *EMBO J.* **6**, 591–598 (1987).
34. M. De Palma, L. Naldini, Tie2-expressing monocytes (TEMs): Novel targets and vehicles of anticancer therapy? *Biochim. Biophys. Acta* **1796**, 5–10 (2009).
35. A. Ehninger, A. Trumpp, The bone marrow stem cell niche grows up: Mesenchymal stem cells and macrophages move in. *J. Exp. Med.* **208**, 421–428 (2011).
36. J. C. Hartner, C. R. Walkley, J. Lu, S. H. Orkin, ADAR1 is essential for the maintenance of hematopoiesis and suppression of interferon signaling. *Nat. Immunol.* **10**, 109–115 (2009).
37. K. Y. King, M. T. Baldrige, D. C. Weksberg, S. M. Chambers, G. L. Lukov, S. Wu, N. C. Boles, S. Y. Jung, J. Qin, D. Liu, Z. Songyang, N. T. Eissa, G. A. Taylor, M. A. Goodell, Irgm1 protects hematopoietic stem cells by negative regulation of IFN signaling. *Blood* **118**, 1525–1533 (2011).
38. B. N. Bidwell, C. Y. Slaney, N. P. Withana, S. Forster, Y. Cao, S. Loi, D. Andrews, T. Mikeska, N. E. Mangano, S. A. Samarajiva, N. A. de Weerd, J. Gould, P. Argani, A. Moller, M. J. Smyth, R. L. Anderson, P. J. Hertzog, B. S. Parker, Silencing of Irf7 pathways in breast cancer cells promotes bone metastasis through immune escape. *Nat. Med.* **18**, 1224–1231 (2012).
39. S. Kurian, M. Qazilbash, J. Fay, S. Wolff, R. Herzig, G. Hobbs, P. Bunner, R. Weisenborn, M. Aya-Ay, J. Lynch, S. Ericson, Complete response after high-dose chemotherapy and autologous hematopoietic stem cell transplantation in metastatic breast cancer results in survival benefit. *Breast J.* **12**, 531–535 (2006).
40. C. Farquhar, J. Marjoribanks, R. Basser, S. Hetrick, A. Lethaby, High dose chemotherapy and autologous bone marrow or stem cell transplantation versus conventional chemotherapy for women with metastatic breast cancer. *Cochrane Database Syst. Rev.* **3**, CD003142 (2005).
41. S. E. Salmon, J. J. Crowley, T. M. Grogan, P. Finley, R. P. Pugh, B. Barlogie, Combination chemotherapy, glucocorticoids, and interferon alfa in the treatment of multiple myeloma: A Southwest Oncology Group study. *J. Clin. Oncol.* **12**, 2405–2414 (1994).
42. F. Lansigan, F. M. Foss, Current and emerging treatment strategies for cutaneous T-cell lymphoma. *Drugs* **70**, 273–286 (2010).
43. P. Baldo, M. Rupolo, A. Compagnoni, R. Lazzarini, A. Bearz, R. Cannizzaro, S. Spazzapan, I. Truccolo, L. Moja, Interferon-alpha for maintenance of follicular lymphoma. *Cochrane Database Syst. Rev.* **1**, CD004629 (2010).
44. A. Follenzi, L. Naldini, Generation of HIV-1 derived lentiviral vectors. *Methods Enzymol.* **346**, 454–465 (2002).
45. M. De Palma, L. Naldini, Transduction of a gene expression cassette using advanced generation lentiviral vectors. *Methods Enzymol.* **346**, 514–529 (2002).
46. M. De Palma, E. Montini, F. R. Santoni de Sio, F. Benedicenti, A. Gentile, E. Medico, L. Naldini, Promoter trapping reveals significant differences in integration site selection between MLV and HIV vectors in primary hematopoietic cells. *Blood* **105**, 2307–2315 (2005).
47. M. De Palma, M. A. Venneri, C. Roca, L. Naldini, Targeting exogenous genes to tumor angiogenesis by transplantation of genetically modified hematopoietic stem cells. *Nat. Med.* **9**, 789–795 (2003).

Acknowledgments: We thank A. Mondino, P. Genovese, A. Giustacchini, and M. Novello for help with some experiments; K. Radford for scientific advice; L. Sergi for vector production; S. Indraccolo for providing the human IFN- α cDNA; B. Camisa for technical help with IL-7 and IL-15 ELISA; E. Ferrero for providing HUVECs; and A. Cimarelli for providing the SIV3⁺ packaging construct for the generation of SIV-like particles. **Funding:** This research was supported by grants from the Associazione per la Ricerca sul Cancro (AIRC IG-10732 to L.N.), the European Research Council (ERC advanced grant TARGETINGGENETHERAPY to L.N.; ERC starting grant TIE2⁺MONOCYTES to M.D.P.), the Italian Ministry of Health (Bando Cellule Staminali to L.N.; Bando Giovani Ricercatori GR-2009-1471693 to A.K.-R.), and “my first AIRC grant” to A.B. **Author contributions:** G.E. performed the research, analyzed the data, and wrote the manuscript; D.M. and A.R. performed the research; P.O.-B. generated MDA3 cell line; M.L.S. generated the hTIE2-IFN LV and performed immunofluorescence staining of human tumors; A.K.-R. developed the monocyte transduction protocol; A.B. helped with the design and interpretation of immunological assays and provided intellectual input; B.G. optimized miRNA regulation for the LVs, provided intellectual input, and edited the manuscript; M.D.P. supervised M.L.S., provided intellectual input, and edited the manuscript; L.N. and R.M. designed and coordinated the research, analyzed the data, and wrote the manuscript. **Competing interests:** The authors declare that they have no competing financial interests. G.E. conducted this study as partial fulfillment of his PhD in molecular and cellular biology at San Raffaele University, Milan, Italy.

Submitted 15 April 2013
Accepted 6 November 2013
Published 1 January 2014
10.1126/scitranslmed.3006353

Citation: G. Escobar, D. Moi, A. Ranghetti, P. Ozkal-Baydin, M. L. Squadrito, A. Kajaste-Rudnitski, A. Bondanza, B. Gentner, M. De Palma, R. Mazziere, L. Naldini, Genetic engineering of hematopoiesis for targeted IFN- α delivery inhibits breast cancer progression. *Sci. Transl. Med.* **6**, 217ra3 (2014).